Journal of Power Sources 196 (2011) 10069–10073

Contents lists available at ScienceDirect

Journal of Power Sources

journal homepage: www.elsevier.com/locate/jpowsour

Short communication

Micro-solid oxide fuel cells using free-standing 3 mol.% yttria-stabilised-tetragonal-zirconia-polycrystal electrolyte foils

Anna Evans*, Anja Bieberle-Hütter, Lorenz J. Bonderer, Stefanie Stuckenholz, Ludwig J. Gauckler

ETH Zurich, Nonmetallic Inorganic Materials, Wolfgang-Pauli-Strasse 10, CH-8093 Zurich, Switzerland

ARTICLE INFO

Article history:
Received 3 February 2011
Received in revised form 28 July 2011
Accepted 31 July 2011
Available online 10 August 2011

Keywords:
TZP
Yttria stabilised zirconia
Ceramic foil
Electrolyte
Micro-solid oxide fuel cell

ABSTRACT

Ultrathin 3 mol.% yttria-stabilised-tetragonal-zirconia-polycrystal (Y-TZP) foils with thicknesses of 1–10 μm are fabricated by a new wet-chemical processing route. The foils are free-standing, semi-transparent and flexible. The in-plane electrical conductivity of the Y-TZP foil is 0.03 S m^{-1} at 500 °C. Cross-plane impedance measurements with sputtered Pt electrodes yield two arcs, of which the high-frequency arc is attributed to the ohmic resistance of the electrolyte and the low-frequency arc to the electrode–electrolyte interface. A symmetrical micro-solid oxide fuel cell (SOFC) is designed using this ultrathin free-standing Y-TZP foil as the electrolyte and sputtered Pt electrodes. An open-circuit voltage of 0.98 V and a maximum power density of 12 mW cm^{-2} are measured at 500 °C. These results prove the feasibility of this approach to the fabrication of miniaturised planar SOFCs without the need for microfabrication.

1. Introduction

Solid oxide fuel cells (SOFCs) are intended for stationary and mobile applications and can be designed with a planar or tubular geometry [1]. For distributed power generation in the kilowatt to megawatt range, the SOFCs are operated at elevated temperatures between 650 °C and 1000 °C to ensure a high ionic conductance of the electrolyte. In planar designs, the electrolyte is a ceramic tape with a thickness of several hundred microns or a thick film of 5–20 μm in the case of anode-supported cells [2]. In tubular designs, the SOFC is electrode-supported with an electrolyte film that is several tens of microns thick. More recently, SOFCs were proposed for portable applications in the watt to kilowatt range, such as leisure cogeneration systems, hybrid electric vehicles and portable devices [3]. Very new research focuses on the development of miniaturised SOFCs, so-called micro-SOFCs, for powering small portable devices in the milliwatt to watt range [4]. Micro-tubular SOFCs consist of millimetre to centimetre long tubes with a diameter down to 100 μm which are bundled together into a stack and can deliver up to 1.1 W cm^{-2} at 600 °C [5–8]. This tubular configuration is highly suitable for short start-up times, and thermal stresses can be minimised. However, problems related to the interconnects and the current collection of micro-SOFC tubes assembled in a stack remain to be solved [5]. Planar micro-SOFCs follow a chip-based approach and are fabricated by micro-electro-mechanical-system (MEMS) techniques which involve processing-intensive, time-consuming and expensive microfabrication steps [4,9–17]. The micro-SOFC membrane consists of a cathode and an anode separated by a dense oxygen-ion conducting electrolyte with a total thickness of ~1 μm. Different microfabricated planar micro-SOFC membrane designs are discussed in the literature [9–17]. However, all designs require a micromachinable substrate, and often only small electrochemically active areas per substrate area can be achieved due to the mechanical stability of the membrane and the anisotropic etching angle of 54.7° in the case of silicon wafers [15]. The resulting free-standing thin-film membranes are rather fragile and are subject to differential stresses between the substrate and the deposited films when heated to the micro-SOFC operation temperature [13]. The thermomechanical stability of the membrane is, however, essential to ensure reliable operation during the thermal cycling of the micro-SOFC.

In this paper, we present a new planar micro-SOFC fabrication approach that does not involve any microfabrication steps but uses ultrathin 1–10 μm thin 3 mol.% yttria-stabilised-tetragonal-zirconia-polycrystal (Y-TZP) free-standing foils fabricated by wet-chemical processing. It should be noted that even though thin films are thinner with typical thicknesses up to several hundred nanometres, we are reporting on foils which better compare to ceramic tapes. Typical tapes are in the range of a few tens to several hundred micrometres and are thus much thicker. Y-TZP was chosen, as it has an increased fracture toughness compared to 8 mol.% yttria-fully-stabilised-zirconia (8YSZ) [18]. However, this foil fabrication route is, in principle, also applicable to 8YSZ. As the ohmic

* Corresponding author. Tel.: +41 44 632 37 63; fax: +41 44 632 11 32.
E-mail address: anna.evans@mat.ethz.ch (A. Evans).

0378-7753/$ – see front matter © 2011 Elsevier B.V. All rights reserved.
doi:10.1016/j.jpowsour.2011.07.087

resistance of these micrometer-thick Y-TZP foils is expected to be only marginally larger than that of the 8YSZ thin-film electrolytes of several hundred nanometres thickness, a SOFC comprising the Y-TZP foil as the electrolyte can be operated in a similar temperature range as typical micro-SOFC membranes. Furthermore, the wafer stack and packaging will only be slightly larger than those for MEMS-based micro-SOFCs.

Another advantage of the Y-TZP foil is the possibility of integrating electrode materials that require annealing temperatures of above 600 °C to obtain the desired microstructural and electrochemical properties. Since the Y-TZP foils are sintered at 1350 °C, these electrolyte foils can be annealed at high temperatures for electrode preparation without any degradation. This is not possible for thin-film yttria-stabilised-zirconia electrolytes in microfabricated micro-SOFCs in which crystallisation, grain growth and the micromachinable substrate (e.g. silicon wafer) have to be taken into consideration, since the thin film electrolytes were processed at low temperatures and will change when annealed at higher temperatures for electrode fabrication.

In the first part of this paper, the fabrication and microstructural characteristics of the Y-TZP foil are described. Then, the electrical and electrochemical properties of the Y-TZP foil are investigated and a symmetrical micro-SOFC based on these Y-TZP electrolyte foils is demonstrated.

2. Experimental

The 12 vol.% Y-TZP powder suspension (3 mol.% yttria-stabilised-tetragonal-zirconia TZ-3Y-E, Tosoh, Japan) with 5 wt.% steric stabiliser sorbitan monooleate (Span80, Fluka, Switzerland) in toluene (Fluka, Switzerland) is ball-milled with 2 mm TZP milling balls for 4 days [19]. The Y-TZP foil is fabricated by off-centred spin-coating (custom-made device, 500 rpm, +100 rpm s^{-1} acceleration, 180 s) of the Y-TZP powder suspension onto a flat-pressed graphite foil substrate (5 cm × 5 cm, Sigraflex® TH, SGL Group, Germany) as described in [19]. The 5 cm × 5 cm green film is sintered in air up to 1350 °C for 2 h (heating and cooling rates of 15 °C min^{-1} and 5 °C min^{-1}, respectively), whereby the graphite foil is burnt off and free-standing 4 cm × 4 cm ultrathin Y-TZP foils with a thickness of 1–10 μm are formed. Further processing details can be found in Ref. [19].

The thickness of the Y-TZP foils was determined both gravimetrically (using the foil area and a density of 6.2 g cm^{-3} for Y-TZP) and from cross-sectional scanning electron microscopy images (SEM, Leo 1530, Carl Zeiss SMT).

The in-plane electrical properties of a 6.8 μm thick Y-TZP foil (1 cm × 3 cm) were measured using a four-point setup [20]. The Y-TZP foil was placed on a sapphire single crystal substrate (Stettler Sapphire AG, Switzerland), and four Pt electrodes (thickness of ~150 nm) were sputtered onto the foil through a shadow mask (SCD 050 Sputter Coater, Bal-Tec, 40 mA, 0.05 mbar, 120 s). On each sputtered Pt stripe, a flat-pressed Pt wire (125 μm diameter) covered with Pt paste (C3605P, Heraeus GmbH, Germany) was placed on the Y-TZP foil and glued to the sapphire substrate with two bonds of ceramic binder (Firag Ebmatingen, Switzerland). The four-point electrical d.c. conductivity measurements were performed using a digital multimeter (197 A, Keithley Instruments, USA). All the conductivity experiments were performed in air as a function of temperature (250–1000 °C) with heating and cooling rates of 3 °C min^{-1}.

The electrochemical characterisation of a 6.7 μm Y-TZP foil electrolyte was carried out by impedance spectroscopy cross-plane measurements. The 1 cm × 1 cm Y-TZP foil was placed on a sapphire single crystal substrate (Stettler Sapphire AG, Switzerland) which had a thin Pt layer sputtered through a 1 cm × 1 cm shadow mask (SCD 050 Sputter Coater, Bal-Tec, 40 mA, 0.05 mbar, 240 s) and was covered with Pt paste. The top electrode was achieved by brushing Pt paste (C3605P, Heraeus GmbH, Germany) onto a flat-pressed Pt-mesh current collector (52 mesh, Alfa Aesar, Germany) which was carefully placed onto the Y-TZP foil and attached with ceramic glue. The impedance data was recorded between 250 °C and 750 °C in steps of 50 °C with heating and cooling rates of 3 °C min^{-1} using an IM6 workstation (Zahner Elektrik, Germany) in a frequency range of 1 Hz to 4 MHz with an a.c. excitation amplitude of 100 mV. All the measurements were performed in air without a bias. The impedance data from the second thermal cycle was used for the evaluation in order to avoid any effects from burning off the Pt paste during the first heating. The impedance data was analysed and fitted using the ZView software (version 3.2c, Scribner Associates, USA).

For the micro-SOFC testing, the 4 cm × 4 cm Y-TZP foil was cut down to 2 cm × 2 cm in order to remove the wrinkled parts on the edge and to use only the middle part which was almost flat. 80 nm Pt electrodes with a diameter of 1 cm were sputtered (PVD Products, USA, 100 W, 75 mTorr Ar, 246 s) onto a 3.0 μm thick 2 cm × 2 cm Y-TZP foil electrolyte. This micro-SOFC was then carefully placed between two 2 cm × 2 cm Foturan® glass ceramic wafers, with a 0.5 cm hole in the bottom piece and a 1 cm hole in the top piece. The Foturan® wafer pieces were etched according to the procedure described in [21]. The micro-SOFC was clamped between two aluminium oxide spacer rings covered with ceramic paper (Fiberfrax FT1, Unifrax, USA) for sealing.

Electrochemical testing was carried out between 250 °C and 550 °C, under air (cathode) and ~3 vol.% humidified N_2:H_2 4:1 (anode). All gas flows (60–500 sccm) were controlled by mass flow controllers (El-Flow, Bronkhorst, Switzerland). The heating and cooling rates were 1 °C min^{-1}. Current collection was performed via flat-pressed 80 μm Pt wires. Electrochemical impedance spectra and current–voltage curves were recorded with an IM6 workstation (Zahner Elektrik, Germany) at the open-circuit voltage (OCV).

3. Results and discussion

The recently developed fabrication technique from our laboratory for the preparation of free-standing ceramic foils was used to make thin 3 mol.% Y-TZP foils [19]. The off-centred spin-coating of the powder suspension onto the 5 cm × 5 cm graphite foil substrates ensured that the resulting green films had a homogenous thickness. After sintering, the Y-TZP foils have dimensions of 4 cm × 4 cm and a thickness of between 1 μm and 10 μm (Fig. 1). The foils are semi-transparent, very flexible, and slightly wrinkled due to the three-dimensional shrinking of the green film during sintering [19]. The foils are easy-to-handle with tweezers as shown in [19] and have an increased mechanical stability compared to the thin-film electrolytes typically used in micro-SOFCs. The SEM cross-sectional image of a 3 μm thin Y-TZP foil sintered at 1350 °C reveals a dense microstructure with round grains of about 300 nm (Fig. 1(b)). Larger grains are related to small chunks originating from the TZP milling balls used for processing of the powder suspension. No thickness gradient within the Y-TZP foils was observed in the cross-sectional SEM images, and the surface roughness is negligible compared to the thickness of the Y-TZP foil.

The electrical characterisation of an Y-TZP foil with a thickness of 6.8 μm was carried out by four-point d.c. in-plane conductivity measurements on a sapphire single crystal (Fig. 2(a)). The Arrhenius-type diagram of the conductivity vs. the inverse temperature is shown in Fig. 2(b). The conductivity of the 3 mol.% Y-TZP foil is 0.03 S m^{-1} at 500 °C. From a linear fit of the data, an activation energy of 1.01 ± 0.03 eV was obtained. These data are in good

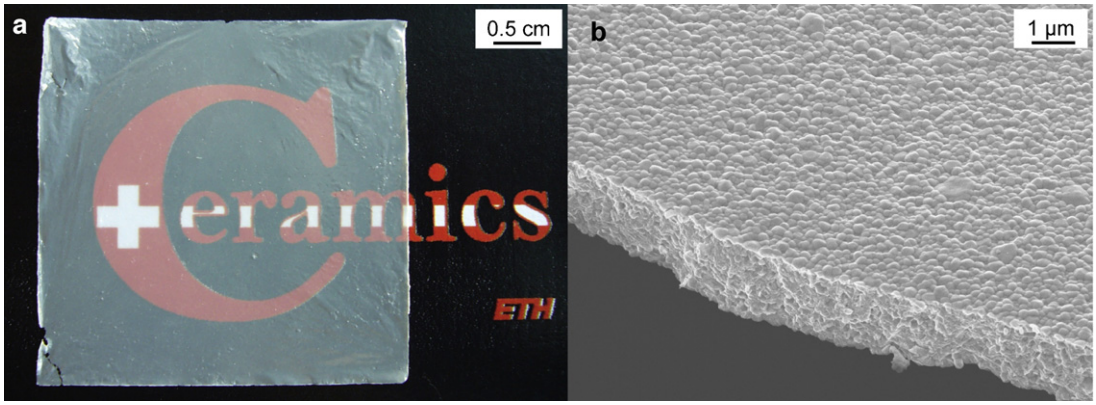

Fig. 1. Free-standing 3 mol.% yttria-stabilised-tetragonal-zirconia-polycrystal (Y-TZP) electrolyte foil with a thickness of 3 μm obtained after sintering at 1350 °C for 2 h. (a) Top-view photograph and (b) tilted scanning electron microscopy cross-sectional image.

agreement with the conductivity from the literature of 3 mol.% Y-TZP bulk and thin films [22]. Literature data for 8YSZ has been added to the diagram since this is the most common electrolyte material used in SOFC – in particular, 8YSZ thin films deposited by pulsed laser deposition and ultrasonic spray pyrolysis which can be integrated into microfabricated micro-SOFCs [22–27]. It can be seen that the literature data for 8YSZ scatters by more than one order of magnitude [23,25–27]; spin-coated thin films by Kosacki et al. [24] show a particularly high conductivity. The scatter is the subject of considerable discussion in the community and can most probably be explained by the fact that different deposition techniques were used – resulting in different micro and nanostructures, such as the degree of crystallinity, grain sizes, porosity, and impurities. The lower ionic conductivity of the Y-TZP foil presented in this study compared to the literature data of 8YSZ is due to the lower concentration of yttria doping (3 mol.% vs. 8 mol.%) [1], the different crystallographic phase (tetragonal vs. cubic), and the larger grain size of 300 nm compared to the 10–200 nm grains in the thin films [22–27]. Furthermore, impurities arising from the sacrificial graphite foil substrate during sintering may also influence the electrical conductivity. It can thus be stated that the measured conductivity of the 3 mol.% Y-TZP foils is as expected from the literature and that the conductivity makes these foils suitable for testing as an electrolyte in a micro-SOFC.

For the electrochemical characterisation of the Y-TZP foil, cross-plane impedance measurements were carried out in a symmetrical cell setup with Pt electrodes (Fig. 3(a)). The impedance spectra recorded between 550 °C and 750 °C are shown in Fig. 3(b) and consist of two arcs in the Nyquist diagram. The spectra are fitted with an equivalent circuit model comprising a resistor (R0) accounting for the wires used for current collection and two resistor – constant phase elements (R1-CPE1 and R2-CPE2). From the area-specific resistance of the high-frequency arc (R1), a conductivity of 0.04 S m^{-1} at 500 °C with an activation energy of 0.99 ± 0.08 eV was obtained for temperatures of between 250 °C and 750 °C. This is in agreement with the d.c. results described above. A capacitance of 10^{-10} F was derived for CPE1 which is typical for the grain boundaries [28]. The high-frequency arc is thus assigned to the ohmic resistance of the Y-TZP electrolyte foil. The low-frequency arc has a resistance (R2) with an activation energy of

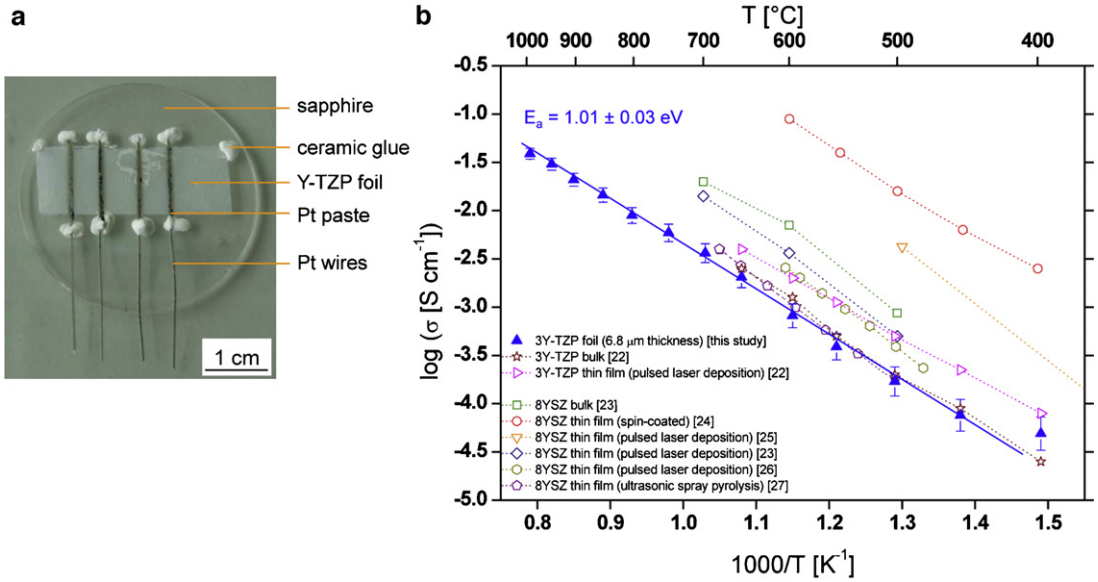

Fig. 2. (a) Top-view photograph of a contacted 3 mol.% yttria-stabilised-tetragonal-zirconia-polycrystal (Y-TZP) foil for a four-point d.c. in-plane conductivity measurement. (b) Arrhenius diagram of the electrical conductivity vs. the inverse temperature of a 3 mol.% Y-TZP foil with a thickness of 6.8 μm. Literature data of 3 mol.% Y-TZP and 8 mol.% yttria-fully-stabilised-zirconia (8YSZ) bulk and thin films is given for comparison [the dashed lines are to guide the eye]. The error bars take into account the heating and cooling cycles. The larger error at lower temperatures is attributed to the burning off of the organics from the Pt paste during the first heating. This data point is thus not considered in the linear fit.

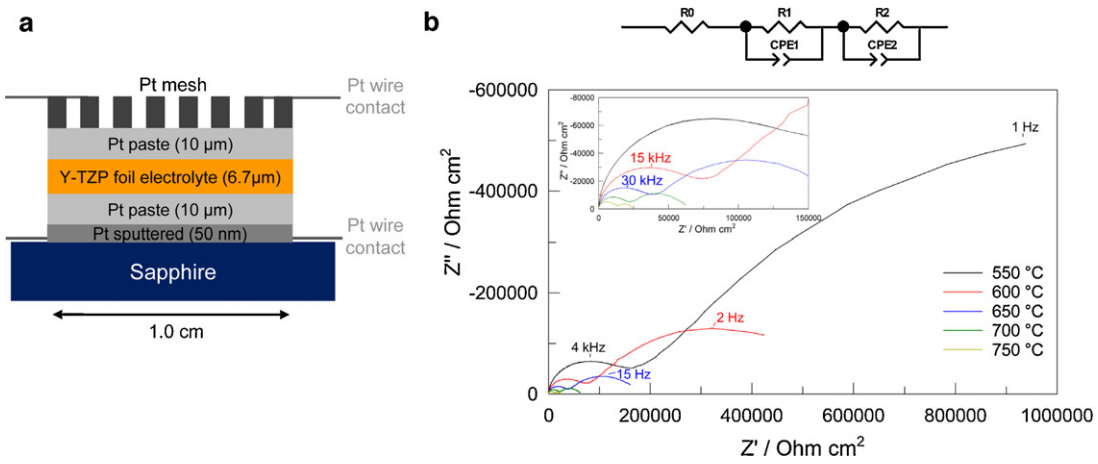

Fig. 3. (a) Schematic representation of the sample design used for a.c. impedance spectroscopy cross-plane measurements. (b) Impedance spectra including selected peak frequencies displayed in a Nyquist diagram for a 6.7 μm Y-TZP foil between 550 °C and 750 °C. The high-frequency area is enlarged in the inset and the equivalent circuit model used for fitting the data is depicted above.

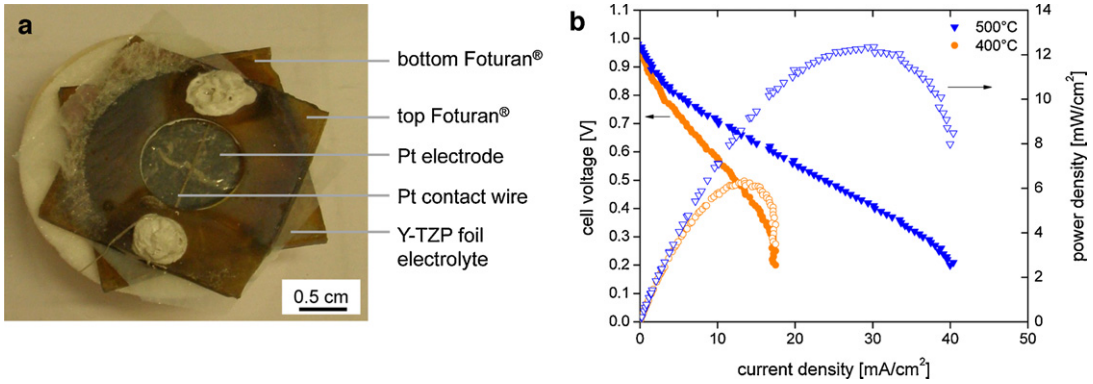

Fig. 4. (a) Photo of the micro-SOFC with the 3.0 μm Y-TZP foil sandwiched between two Foturan® wafer pieces. (b) Micro-SOFC voltage (filled symbols) and power density (empty symbols) vs. current density curves.

1.6 ± 0.3 eV and a capacitance of $\sim 10^{-7}$ F (CPE2), and is attributed to the electrolyte–electrode interface [28].

A 3.0 μm free-standing Y-TZP foil as the electrolyte with 80 nm Pt thin-film electrodes deposited by magnetron sputtering were used to make a micro-SOFC without any microfabrication steps. This trilayer structure is sandwiched between two Foturan® wafers for mechanical support and with a hole to ensure gas access to the electrodes (Fig. 4(a)). Unlike the self-supporting thick ceramic tapes that are used in conventional SOFC, the free-standing Y-TZP foil needs to be kept in place within the test rig, and the key advantage of a Foturan® support is that it has a coefficient of thermal expansion of $\alpha_{\text{Foturan}} = 8.6 \times 10^{-6}\,\text{K}^{-1}$ [21] which is close to that of the Y-TZP foil electrolyte with $\alpha_{\text{TZP}} = 10.6 \times 10^{-6}\,\text{K}^{-1}$, and thus differential stresses are minimised.

The electrochemical testing yielded an open circuit voltage (OCV) of 0.98 V at 500 °C which is similar to microfabricated micro-SOFCs [10,11,16] and comes close to the theoretical OCV of 1.1 V given by the Nernst equation [29]. This OCV value is very high considering that the electrolyte foil is only 3 μm thick and that pinholes are a common issue with traditional ceramic processing. The slight decrease compared to the theoretical value possibly arises from some gas cross-over due to small pinholes in the foil. The maximum power density is 12 mW cm^{-2} at 500 °C (Fig. 4(b)) and demonstrates that a micro-SOFC can be built from these newly processed ultrathin ceramic foils. The electrochemical performance is, however, lower than some power densities of several hundred to one thousand mW cm^{-2} reported for the best microfabricated micro-SOFCs at the same temperature [9–17]. This is mainly due to the degradation of the thin Pt electrodes at 500 °C, but also due to the non-theoretical OCV and the slightly higher ohmic resistance of the Y-TZP foil electrolyte. Post-analysis by SEM of the Pt thin films on the cathode and especially the anode side revealed an agglomerated microstructure that still had in-plane connectivity similar to [30]. This is in agreement with very recent observations regarding the microstructural degradation of thin Pt electrodes upon thermal treatment [11,30–33]. The next micro-SOFCs based on the Y-TZP foil electrolyte will use optimised Pt, e.g. in the form of PtNi, as well as perovskite electrodes such as lanthanum–strontium–cobalt oxide (LSC) or lanthanum–strontium–cobalt–iron oxide (LSCF) [33–35].

These micro-SOFCs with a Y-TZP foil electrolyte also have the advantage of a high surface area utilisation of over 50%, as only the outer edge of the foil has to be supported. The limit of surface area utilisation is currently restricted primarily by the large-area application of the electrodes. For microfabricated micro-SOFCs based on Si wafer, the surface utilisation is much lower: a 350 μm thick Si wafer with free-standing membranes of 100 μm × 100 μm has a poor surface area coverage of 2.8% considering a wet etching angle of 54.7° for KOH etching of Si [15].

4. Conclusions

The recently developed fabrication technique yields free-standing Y-TZP electrolyte foils by wet-chemical processing with dimensions of 4 cm × 4 cm and thicknesses of between 1 μm and 10 μm. These Y-TZP foils have a sufficient mechanical stability to

yield free-standing electrolyte membranes in micro-solid oxide fuel cells, have a much larger area and are easier to handle than the electrolyte thin films in micro-SOFCs. The d.c. in-plane conductivity is 0.03 S m^{-1} at 500 °C and therefore very similar to the conductivity of 8YSZ thin films which are typically used in microfabricated micro-SOFCs. Cross-plane a.c. impedance measurements yielded spectra with two arcs. The high-frequency arc was assigned to the ohmic resistance of the Y-TZP foil, which is in a similar range to the d.c. measurements; and the low frequency arc was attributed to the electrolyte–electrode interface. A feasibility study showed that a micro-SOFC can be built on the basis of these free-standing Y-TZP foils spanning openings of 5 mm. An OCV of 0.98 V and a maximum power density of 12 mW cm^{-2} at 500 °C proved the feasibility of this new approach for future micro-SOFC development. A high surface area utilisation and no need for expensive thin film deposition or microfabrication techniques makes this approach very attractive compared to standard thin film micro-SOFC membrane fabrication routes.

Acknowledgments

The authors thank Barbara Scherrer, Jennifer L.M. Rupp and Michel Prestat for detailed discussions. Financial support is gratefully acknowledged for the ONEBAT project from the Competence Centre for Energy and Mobility (CCEM), Swiss Electric Research (SER), and the Swiss National Foundation (SNF) in the frame of the Sinergia project.

References

[1] S.C. Singhal, K. Kendall, High Temperature Solid Oxide Fuel Cells – Fundamentals, Design and Application, Elsevier Advanced Technology, Oxford, 2003.
[2] J.W. Kim, A.V. Virkar, K.Z. Fung, K. Mehta, S.C. Singhal, J. Electrochem. Soc. 146 (1999) 69.
[3] G.A. Tompsett, C. Finnerty, K. Kendall, T. Alston, N.M. Sammes, J. Power Sources 86 (2000) 376.
[4] A. Bieberle-Hutter, D. Beckel, A. Infortuna, U.P. Muecke, J.L.M. Rupp, L.J. Gauckler, S. Rey-Mermet, P. Muralt, N.R. Bieri, N. Hotz, M.J. Stutz, D. Poulikakos, P. Heeb, P. Muller, A. Bernard, R. Gmur, T. Hocker, J. Power Sources 177 (2008) 123.
[5] K.S. Howe, G.J. Thompson, K. Kendall, J. Power Sources 196 (2011) 1677.
[6] T. Suzuki, M.H. Zahir, T. Yamaguchi, Y. Fujishiro, M. Awano, N. Sammes, J. Power Sources 195 (2010) 7825.
[7] T. Suzuki, Z. Hasan, Y. Funahashi, T. Yamaguchi, Y. Fujishiro, M. Awano, Science 325 (2009) 852.
[8] T. Suzuki, Y. Funahashi, T. Yamaguchi, Y. Fujishiro, M. Awano, J. Power Sources 183 (2008) 544.
[9] A. Evans, A. Bieberle-Hütter, J.L.M. Rupp, L.J. Gauckler, J. Power Sources 194 (2009) 119.
[10] U.P. Muecke, D. Beckel, A. Bernard, A. Bieberle-Hütter, S. Graf, A. Infortuna, P. Müller, J.L.M. Rupp, J. Schneider, L.J. Gauckler, Adv. Funct. Mater. 18 (2008) 1.
[11] K. Kerman, B.-K. Lai, S. Ramanathan, J. Power Sources 196 (2011) 2608.
[12] A.C. Johnson, A. Baclig, D.V. Harburg, B.K. Lai, S. Ramanathan, J. Power Sources 195 (2010) 1149.
[13] I. Garbayo, A. Tarancon, J. Santiso, F. Peiro, E. Alarcon-Llado, A. Cavallaro, I. Gracia, C. Cane, N. Sabate, Solid State Ionics 181 (2010) 322.
[14] S. Rey-Mermet, P. Muralt, Solid State Ionics 179 (2008) 1497.
[15] P.C. Su, C.C. Chao, J.H. Shim, R. Fasching, F.B. Prinz, Nano Lett. 8 (2008) 2289.
[16] H. Huang, M. Nakamura, P.C. Su, R. Fasching, Y. Saito, F.B. Prinz, J. Electrochem. Soc. 154 (2007) B20.
[17] S. Kang, P.C. Su, Y.I. Park, Y. Saito, F.B. Prinz, J. Electrochem. Soc. 153 (2006) A554.
[18] R.H.J. Hannink, P.M. Kelly, B.C. Muddle, J. Am. Ceram. Soc. 83 (2000) 461.
[19] L.J. Bonderer, P.W. Chen, P. Kocher, L.J. Gauckler, J. Am. Ceram. Soc. 93 (2010) 3624.
[20] J.L.M. Rupp, L.J. Gauckler, Solid State Ionics 177 (2006) 2513.
[21] T.R. Dietrich, W. Ehrfeld, M. Lacher, M. Kramer, B. Speit, Microelectron. Eng. 30 (1996) 497.
[22] S. Heiroth, T. Lippert, A. Wokaun, M. Dobeli, J.L.M. Rupp, B. Scherrer, L.J. Gauckler, J. Eur. Ceram. Soc. 30 (2010) 489.
[23] J.H. Joo, G.M. Choi, Solid State Ionics 177 (2006) 1053.
[24] I. Kosacki, T. Suzuki, V. Petrovsky, H.U. Anderson, Solid State Ionics 136 (2000) 1225.
[25] A. Infortuna, A.S. Harvey, L.J. Gauckler, Adv. Funct. Mater. 18 (2008) 127.
[26] S. Heiroth, T. Lippert, A. Wokaun, M. Döbeli, Appl. Phys. A: Mater. Sci. Process. 93 (2008) 639.
[27] M.F. García-Sánchez, J. Peña, A. Ortiz, G. Santana, J. Fandiño, M. Bizarro, F. Cruz-Gandarilla, J.C. Alonso, Solid State Ionics 179 (2008) 243.
[28] J.T.S. Irvine, D.C. Sinclair, A.R. West, Adv. Mater. 2 (1990) 132.
[29] S.W. Zha, C.R. Xia, G.Y. Meng, J. Appl. Electrochem. 31 (2001) 93.
[30] T. Ryll, H. Galinski, L. Schlagenhauf, P. Elser, J.L.M. Rupp, A. Bieberle-Hutter, L.J. Gauckler, Adv. Funct. Mater. 21 (2011) 565.
[31] H. Galinski, T. Ryll, P. Elser, J.L.M. Rupp, A. Bieberle-Hutter, L.J. Gauckler, Phys. Rev. B 82 (2010) 11.
[32] Y.B. Kim, C.M. Hsu, S.T. Connor, T.M. Gur, Y. Cui, F.B. Prinz, J. Electrochem. Soc. 157 (2010) B1269.
[33] X.H. Wang, H. Huang, T. Holme, X. Tian, F.B. Prinz, J. Power Sources 175 (2008) 75.
[34] B.-K. Lai, K. Kerman, S. Ramanathan, J. Power Sources 196 (2011) 1826.
[35] H.-S. Noh, H. Lee, H.-I. Ji, H.-W. Lee, J.-H. Lee, J.-W. Son, J. Electrochem. Soc. 158 (2011) B1.